JOURNAL OF VIROLOGY, July 2011, p. 7108–7117 Vol. 85, No. 14
0022-538X/11/$12.00 doi:10.1128/JVI.00573-11

Identification of Amino Acid Residues Important for Heparan Sulfate Proteoglycan Interaction within Variable Region 3 of the Feline Immunodeficiency Virus Surface Glycoprotein▽

Qiong-Ying Hu, Elizabeth Fink, Meaghan Happer, and John H. Elder*

Department of Immunology and Microbial Science, The Scripps Research Institute, La Jolla, California

Received 22 March 2011/Accepted 28 April 2011

Heparan sulfate proteoglycans (HSPGs) act as binding receptors or attachment factors for the viral envelope of many viruses, including strains of HIV and feline immunodeficiency virus (FIV). The FIV gp95 glycoprotein (SU) from laboratory-adapted strains (tissue culture adapted [TCA]) such as FIV-34TF10 can bind to HSPG, whereas SU from field strains (FS) such as FIV-PPR cannot. Previous studies indicate that SU-HSPG interactions occur within the V3 loop. We utilized a series of nested V3 peptides to further map the HSPG binding sites and found that both sides of the predicted V3 loop stem were critical for the binding but not the CXCR4 binding domain near the predicted tip of the V3 loop. Neutralization assays for TCA strain entry using the same set of V3 peptides showed that peptides targeting CXCR4 or HSPG binding sites can block infection, supporting the V3 loop as a critical neutralization target. Site-directed mutagenesis identified two highly conserved arginines, R379 and R389, on the N-terminal side of the V3 stem as critical for the contact between SU and HSPG. Residues K407, K409, K410, and K412 on the C-terminal side of the V3 stem form a second nonconserved domain necessary for HSPG binding, consistent with the observed specificity distinctions with FS FIV. Our findings discriminate structural determinants important for HSPG and CXCR4 binding by FIV SU and thus further define the importance of the V3 loop for virus entry and infection.

Feline immunodeficiency virus (FIV) causes an AIDS-like disease in its natural host, the domestic cat (37), and is thus a valuable animal model for the development of antiviral agents against lentivirus infections, including human immunodeficiency virus (HIV); design of anti-HIV vaccines; and study of lentiviral pathogenesis (11, 40, 56, 60). To date, four different cell surface molecules that interact with FIV SU have been identified: CXCR4 (9, 41, 59, 61), CD134 (6, 48), heparan sulfate proteoglycan (HSPG) (7, 9), and DC-SIGN (9, 10). The chemokine receptor CXCR4 is used as a common entry receptor by FIV of domestic cats (9, 41, 59, 61). Feline CD134 acts as the primary binding receptor for FIV entry into host cells, a function that parallels use of CD4 as a primary receptor in HIV infection (6, 48). Binding of CD134 alters the conformation of FIV SU and promotes high-affinity binding to CXCR4. HSPG, a type of glycosaminoglycan (GAG) consisting of a core protein with O-linked heparan sulfate polysaccharide chains, has a ubiquitous tissue expression but is predominantly expressed on epithelial cells and astrocytes (7, 9, 23) and is critical for the cellular attachment of many viruses (50), including herpesvirus (1), flavivirus (19), adenovirus (54), papillomavirus (45), and certain retrovirus family members, including certain strains of HIV and FIV (3, 7, 10, 43). DC-SIGN, a cell surface C-type lectin expressed on dendritic cells (DCs), is thought to play key roles in the interaction of DCs with T cells as well as in HIV and FIV pathogenesis (16). Binding properties of FIV SU for each of these receptors are dependent on the origin of SU. Therefore, it is important to analyze all the known receptor interactions with SU obtained from distinct origins and map the regions of SU involved in CXCR4, CD134, HSPG, and DC-SIGN receptor binding. Knowledge gained can then be used to develop mechanism-driven intervention strategies applicable to blocking both FIV and HIV infections. Although FIV SU interaction with CXCR4 has been well documented (20, 52), the role played by other receptors and the binding domains of SU for each receptor are less clear.

Our previous studies showed that HSPG, in conjunction with CXCR4, could facilitate infection by laboratory-adapted strains (tissue culture adapted [TCA]) of adherent, CD134-negative cell lines such as CrFK and G355-5. The prototype TCA isolate for our studies, termed FIV-34TF10, was cloned from FIV-Petaluma virus that had been adapted to growth on CrFK cells (53). In contrast, SU from field strains (FS) of FIV cannot bind to HSPG (7, 9) or productively infect adherent ($CD134^-$ $CXCR4^+$) cell lines. As demonstrated by FIV-34TF10, FS FIV could, however, be adapted for growth on CrFK cells and adaptation correlated with the ability of SU to bind HSPGs. Therefore, we wished to identify the determinants in SU encoded by TCA FIV for interaction with HSPG and to explore the mechanism of the facilitator role of HSPG for infection.

Several methodologies have been used to study HSPG interactions, including mapping using synthetic peptides (21, 34), site-directed mutagenesis (17, 47, 62), molecular modeling (2, 4, 30, 47, 51), high-resolution nuclear magnetic resonance (NMR) spectroscopy (2, 25, 47), X-ray crystallography (24, 33, 46), and hydrodynamic measurements (28). An early work based on heparin binding protein sequence comparisons in HIV-1 led to the proposition that two consensus heparin binding sequences, XBBXBX and XBBBXXBX motifs (where B

* Corresponding author. Mailing address: Department of Immunology and Microbial Science, The Scripps Research Institute, 10550 North Torrey Pines Road, MB-14, La Jolla, CA 92037. Phone: (858) 784-8270. Fax: (858) 784-2750. E-mail: jelder@scripps.edu.

▽ Published ahead of print on 4 May 2011.

stands for a basic and X for a neutral/hydrophobic amino acid), dictated such interactions (4). However, the universality of this paradigm has been challenged by analysis of additional HSPG ligands. Site-directed mutagenesis (17, 47, 62), molecular modeling (2, 30, 47, 51), NMR (2, 25, 47), and structural characterization of protein-heparin complexes by X-ray crystallography (24, 33) indicate that HSPG binding sites are not exclusively composed of linear sequences and can also include conformational epitopes comprising distant amino acids organized in a precise spatial orientation through the folding of the protein (58).

TCA FIV has been shown to have particular mutations whereby one or two glutamate residues (407 and 409) have been replaced by lysine residues in the V3 loop (35, 49, 53, 57). Results reported here show that adaptation of FIV-PPR for propagation in CrFK cells also involves, among others, a specific change of glutamate to lysine at position 407 within the V3 loop. Furthermore, the results showed that both the N-terminal and the C-terminal sides of the V3 stem-loop are critical for HSPG binding, distinct from CXCR4 binding site at the predicted tip of the V3 loop.

MATERIALS AND METHODS

Cell lines, virus, and reagents. CrFK cells were obtained from the American Type Culture Collection (ATCC, Manassas, VA), and the feline glial cell line (G355-5) was kindly provided by Don Blair (National Institutes of Health, Bethesda, MD). These cells are interleukin-2 (IL-2)-independent adherent cells with high heparin sulfate proteoglycan (HSPG) expression and low CXCR4 expression and are negative for CD134 expression (7, 9). The IL-2-independent feline lymphoma cell line 3201 was obtained from William Hardy (Sloan-Kettering Memorial Hospital, New York, NY). 3201 cells have high CXCR4 expression, with very low or negative expression of CD134 and HSPG (9). The continuous T-cell line 104-C1 was isolated from feline peripheral blood mononuclear cells (PBMC) by limiting dilution; this cell line has high CD134 expression but low CXCR4 and HSPG expression (9). CHO-K1, CHO-pgsA745, and 293T cells were purchased from the ATCC. CHO-K1 cells express HSPG (9, 10), while the mutant CHO-K1 cell line CHO-pgsA745 is defective in the biosynthesis of glycosaminoglycans and thus does not express HSPG (9, 10). Propagation of the different cell lines was performed as previously described (7, 20, 27, 52). The FIV field strain used in the present study, FIV-PPR, is a molecular clone of the clade A San Diego isolate (39). PPR_{CrFK} (PPRcr) is an FIV-PPR strain obtained after *ex vivo* passage in the CrFK cell line (see below), with expanded host cell range (7). FIV-34TF10 is a molecular clone of the FIV-Petaluma isolate that had been adapted for growth on CrFK cells (53). Heparin, AMD3100, and bovine serum albumin (BSA) were purchased from Sigma (St. Louis, MO).

Generation of FIV-PPR_{CrFK}. Continuous passage of FIV-PPR on CrFK cells ($CD134^{Negative}$ $CXCR4^{Low}$) for a period of approximately 3 weeks resulted in the outgrowth of virus, termed FIV-PPR_{CrFK} (PPRcr), that could also be propagated in G355-5 cells ($CD134^{Neg}$ $CXCR4^{Low}$). To generate a molecular clone, CrFK cells were acutely infected with FIV-PPRcr. The envelope gene was amplified from cDNA prepared from infected CrFK cells and then cloned into FIV-PPR in pUC119 vector as previously described (26). The envelope of FIV-PPRcr was amplified by reverse transcriptase PCR (RT-PCR; Stratagene, La Jolla, CA) with the primers 5′-CCCATTTAGAGTACCTGCAG-3′ (6382 to 6401) and 5′-CGA ATAGTTTTCTGAAGCGGTCTTCTAAATCTGTCATCAT-3′ (9001 to 9040), and the full-length construct was sequenced.

Recombinant SU proteins. Expression plasmids encoding SU of FIV-PPR, FIV-PPRcr, and FIV-34TF10 were constructed and used for production of stable CHO-K1 cell lines, as previously described (7, 8). Single colonies with high expression of desired Fc-tagged proteins were selected, and SU-Fc fusion proteins (adhesins) were purified as described previously (20) and quantified using a human IgG enzyme-linked immunosorbent assay (ELISA) quantitation kit (Bethyl Laboratories, Inc., Montgomery, TX). Finally, relative quantitation of proteins was confirmed by Western blot analysis, as previously described (20).

Flow cytometry analysis. Binding of SU-Fc adhesins or Fc (negative control) to the surfaces of G355-5, CrFK, CHO, 3201, or 104-C1 cells was detected using a phycoerythrin (PE)-conjugated goat anti-human IgG1 Fc antibody (MP Biomedicals, Aurora, OH) and analyzed by flow cytometry, using FlowJo software (Tree Star, San Carlos, CA). Briefly, for the binding to G355-5 cells (or other cells for HSPG binding detection), 1×10^5 cells were incubated at 4°C for 30 min in the presence or absence of V3 peptides and then spun down to remove the peptides and washed twice; PPR, PPRcr, or 34TF10 SU-Fc (500 ng) in Earle's balanced salt solution (EBSS)-0.1% bovine serum albumin was added to cells and incubated at 4°C for 45 min. After washing, cells were labeled with a 1:1,000 dilution of PE-conjugated goat anti-human IgG1 antibody for 35 min at 4°C. SU-Fc binding was monitored by fluorescence-activated cell sorting (FACS) analysis. CXCR4-specific binding was confirmed by pretreatment of cells with the CXCR4 antagonist AMD3100 at 0.3 μg/ml for 30 min at 4°C, followed by the incubation with SU-Fc adhesins for 45 min at 4°C. HSPG-specific binding was confirmed by coincubation with SU-Fc adhesins plus heparin (10 μg/ml) for 45 min at 4°C and analyzed as above. For binding to 3201 or 104-C1 cells, the process was the same, except that 2×10^5 cells and 100 ng of SU-Fc were used and the procedure was performed in EBSS-2% fetal bovine serum (FBS) buffer at 25°C. Percent inhibition was calculated by the formula $100 - [(t - c)/(m - c) \times 100]$, where t represents the signal for the test sample, c represents the background signal in the absence of SU-Fc, and m represents the signal obtained for SU-Fc in the absence of peptides or inhibitors.

Peptide synthesis. Peptides were synthesized on a PTI Symphony multiple peptide synthesizer utilizing standard 9-fluorenylmethoxy carbonyl (FMOC) chemistry. Crude peptide material was purified by high-pressure liquid chromatography, and the purity was determined to be greater than 90% on all materials. Mass of peptides was confirmed by mass spectrometry. All the peptides were dissolved in dimethyl sulfoxide (DMSO) at 5 mg/ml as stock solutions. All peptides used in this study have been previously used and reported in mapping studies to define the CXCR4 binding region within V3 (52), with the exception of SU2 (QRNRWEWRPDFKSKKVKISLPC), which had been previously prepared as a potential immunogen for antibody preparation.

Construction of mutant plasmids. Mutations were introduced into a cytomegalovirus-FIV hybrid vector (pCFIV) (22) using the QuikChange site-directed mutagenesis strategy (Stratagene, La Jolla, CA) as recommended by the manufacturer. The presence of the desired mutations and the absence of any other mutations were confirmed by DNA sequencing.

Virus entry assay. pCFIV hybrid vectors pseudotyped with FIV-34TF10 envelope genes or mutants with substitutions for specific amino acids were cotransfected with a beta-galactosidase (β-Gal)-expressing packaging vector in 293T cells (22). Two days later, viral supernatants were collected and each pseudovirion was assessed for the level of reverse transcriptase (RT) for core expression and also an ELISA using antibodies against the V3 region of SU to detect the expression of SU. Both RT assay and ELISA indicated that each envelope construct was well expressed. RT activity is further used as an internal quantitation to normalize transfection efficiency and further to ensure input of approximately equal numbers of pseudovirions. Thus, RT values were normalized to 50,000 cpm per infection before a single-round infection assay was performed in G355-5 cells. After 48 h of infection, β-Gal activity was measured with the Tropix Galacto-Star chemiluminescent reporter gene assay (Applied Biosystems, Carlsbad, CA) according to the manufacturer's guidelines. For neutralization studies, peptides used at final concentrations of 25 μg/ml were preincubated with G355-5 cells for 60 min at 37°C and then cotreated with 34TF10 pseudovirions and cells were assayed for beta-galactosidase expression as described above.

Micro-RT activity assay. The micro-RT activity assay was performed as previously described (7, 8, 52). Briefly, 50 μl of cell-free supernatant together with 10 μl of lysis buffer (0.75 M KCl, 20 mM dithiothreitol, 0.5% Triton X-100) was incubated at room temperature for 10 min. Then, 40 μl of a mixture containing 125 mM Tris-HCl (pH 8.1), 12.5 mM $MgCl_2$, 1.25 μg poly(rA)-poly$(dT)_{12–18}$ (Amersham Biosciences, Piscataway, NJ), and 1.25 μCi of [^{3}H]dTTP (DuPont, Boston, MA) was added to the sample followed by 2 h of incubation at 37°C. Quantitation of RT activity was previously described (8).

RESULTS

Sequence changes associated with HSPG binding. Passage of FS FIV on the adherent cell line CrFK or G355-5 eventually results in the outgrowth of virus adapted to productive growth on either cell line (26, 27). FIV-PPR_{CrFK} (FIV-PPRcr) emerged after passage of FIV-PPR through CrFK cells. The envelope of FIV PPRcr was sequenced, revealing nine amino acid substitutions relative to wild-type FIV-PPR (Fig. 1). Sub-

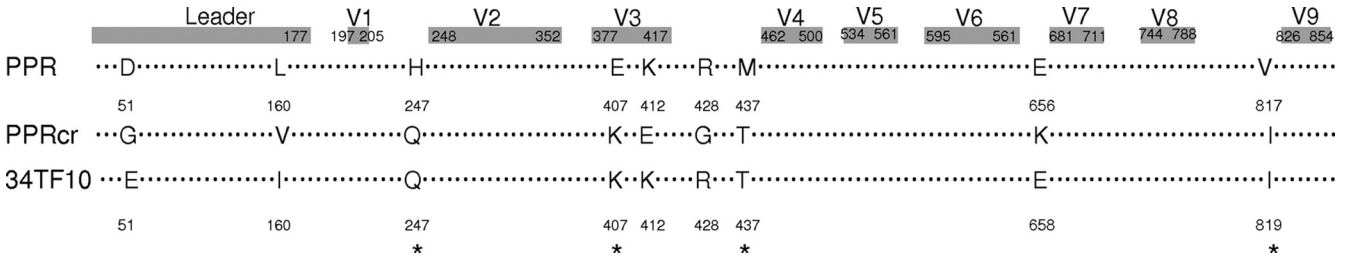

FIG. 1. Schematic representation of sequence alignment of PPR, PPRcr, and 34TF10 SU glycoprotein. A total of nine mutations were noted between FS FIV-PPR and TCA FIV-PPRcr. Six of the above nine amino acid positions were the same in TCA FIV-34TF10 as in FIV-PPR, and four of the six changes were common between the two TCA isolates.

stitutions included changes Asp51Gly and Leu160Val in the region N terminal to the membrane leader sequence, His247Gln in C2, Glu407Lys and Lys412Glu in V3, Arg428Gly and Met437Thr in C3, Glu656Lys between the polar domain and the leucine zipper of TM, and Val817Ile in the cytoplasmic tail. Comparison with another TCA isolate, FIV-34TF10, showed that six of the above nine amino acid positions also were changed relative to FIV-PPR and four of the six changes were common between the two TCA isolates (Fig. 1). In addition, 34TF10 has other differences in the envelope (Env) from parent PPR, which may in some way contribute to adaptation for tissue culture propagation of 34TF10 independent of HSPG binding.

PPRcr SU-Fc can bind to HSPG-expressing cells. To determine if the adaptation of TCA FIVs for productive growth in CrFK cells was caused by the acquired ability of SU to bind to HSPG, we compared the binding characteristics of PPR, PPRcr, and 34TF10 SU-Fc immunoadhesins on G355-5 and CrFK cells (both cell types are $HSPG^{High}$ $CXCR4^{Low}$ $CD134^{Neg}$) (Fig. 2). SU-Fc immunoadhesins corresponding to each virus envelope were quantified by Western blot analysis (data not shown) and then employed in FACS analyses on $HSPG^{+}$ indicator cells. Consistent with past observations (7), PPR SU-Fc could not bind to G355-5 (Fig. 2, top left panel) or CrFK (Fig. 2, middle left panel) cells, but PPRcr SU-Fc bound to both cell lines (top and middle right panels, respectively). Furthermore, the binding of PPRcr SU-Fc could be inhibited by heparin but not the CXCR4 antagonist AMD3100, affirming that the binding observed in this assay was via HSPG interaction rather than CXCR4. Further verification of the nature of SU binding was obtained by comparing SU binding characteristics of CHO-K1 cells ($HSPG^{High}$ $CD134^{Neg}$ $CXCR4^{Neg}$) to those of the CHO mutant cell line pgsA745, which is defective in the biosynthesis of glycosaminoglycans and thus does not express HSPG (10, 13). The results of FACS analysis demonstrate that PPRcr SU-Fc readily bound to CHO-K1 cells, with binding blocked by heparin (Fig. 2, bottom left panel). In contrast, there was no measurable binding detected on pgsA745 cells (Fig. 2, bottom right panel).

Results of binding studies on 3201 ($CXCR4^{High}$ $HSPG^{Neg}$ $CD134^{Neg}$) cells, where the detectable FACS binding is primarily via CXCR4, indicated that blocking of CXCR4 binding by PPRcr occurs in the presence of heparin (Fig. 3). Whereas heparin had little influence on wild-type PPR SU binding to these cells (Fig. 3A), substantial interference was noted for binding by TCA PPRcr SU (Fig. 3B). Primary binding by both envelope proteins occurs via CXCR4, as attested by blocking with AMD3100 (data not shown). These findings are consistent with the close proximity of the two HSPG and CXCR4 binding regions and indicate that steric blocking occurs with heparin binding to TCA FIV that interferes with both interactions.

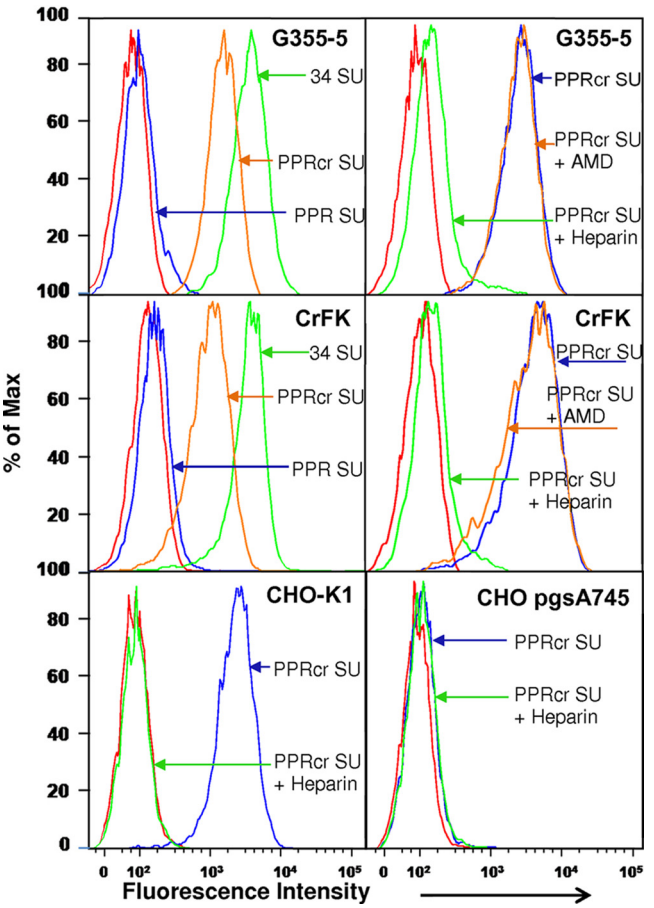

FIG. 2. PPRcr SU can bind to HSPG-expressing cells. FACS analysis of FIV SU binding to G355-5 cells (top), CrFK (middle), CHO-K1 (bottom left), and CHO-pgsA745 (bottom right). Cells were preincubated with the CXCR4 antagonist AMD3100 (0.3 μg/ml) at 4°C for 30 min prior to incubation with SU or coincubated with SU and heparin (10 μg/ml) at 4°C for 45 min. After washing, FIV SU-Fc binding was measured by using a phycoerythrin-conjugated anti-Fc antibody and then monitored by FACS analysis. Results are representative of three independent determinations.

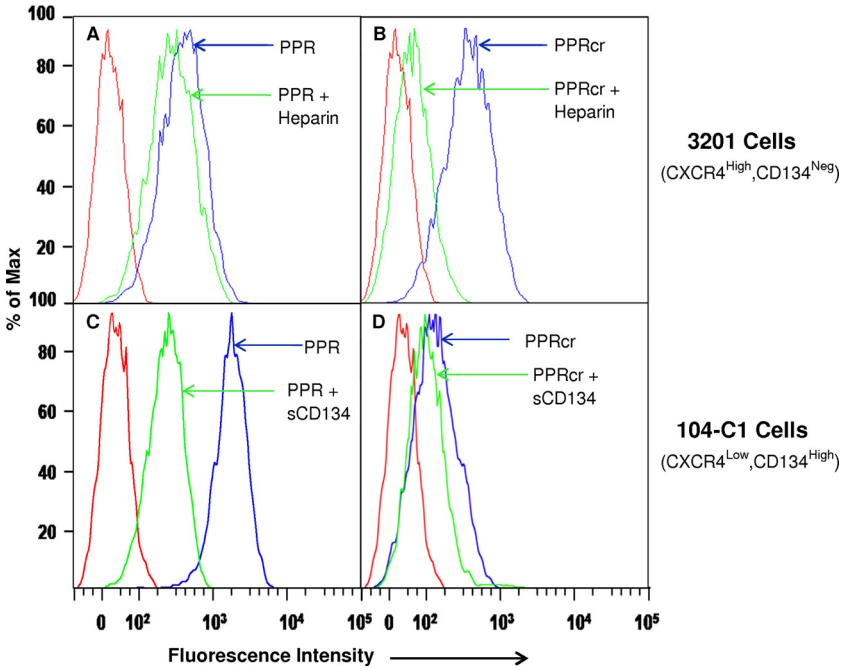

FIG. 3. Comparative binding of PPR and PPRcr SU to CXCR4 (3201 cells) and CD134 (104-C1 cells). (A) FS PPR SU binding to CXCR4 on 3201 cells with or without heparin. (B) TCA PPRcr SU binding to CXCR4 on 3201 cells with or without heparin. (C) FS PPR SU binding to CD134 on 104-C1 cells with or without soluble CD134 (sCD134) as competitor. (D) TCA PPRcr SU binding to CXCR4 with or without soluble CD134 as competitor. Heparin in panels A and B was incubated with SU for 45 min at 25°C, at 20 μg/ml. Soluble CD134 (25 μg/ml) in panels C and D was incubated with SU at 25°C for 30 min prior to addition to cells and then incubated for another 45 min, washed, and analyzed by FACS. Results are representative of three independent determinations.

An assessment of the relative binding of FS and TCA SU to the primary binding receptor, CD134, on 104-C1 ($CD134^{High}$ $HSPG^{Low}$ $CXCR4^{Low}$) cells (Fig. 3C and D) revealed that binding was markedly reduced with PPRcr SU (Fig. 3D) relative to wild-type PPR SU (Fig. 3C). Binding to CD134 still occurred with TCA SU, but the binding was much weaker than with FS SU at concentrations that yielded the same level of binding to CXCR4 on 3201 cells (Fig. 3A and B).

Both N-terminal and C-terminal sides of the V3 loop are critical for the HSPG binding. Previous research (35, 49, 53, 57) indicated that CrFK tropism determinants are associated with the putative V3 loop. Therefore, we tested a series of synthetic V3 peptides encompassing the whole or part of the 41-amino-acid-long V3 loop for ability to block TCA SU binding to HSPG (Table 1). Full-length V3 peptide inhibited binding of PPRcr SU-Fc or 34TF10 SU-Fc to HSPG in a dose-dependent manner (data not shown), indicating that the V3 loop is involved in HSPG binding and contains binding determinants. A panel of nested peptides that overlap the entire V3 exhibited various capacities to interfere with the SU-HSPG binding (Table 1). Interestingly, peptides N190, N212, and N158, which block SU binding to CXCR4 (52), had little effect on HSPG binding (Table 1). Even the potent CXCR4 inhibitors N43 and N44 (52) had only a modest effect on HSPG binding (Table 1). The peptides spanning the N43 region truncated at their N termini, such as N156 and N157, exhibited no effect on HSPG binding (Table 1). Thus, the CXCR4 binding region at the tip (top of the predicted loop structure) of V3 is not directly involved in HSPG interaction. In contrast, peptides on either side of the CXCR4 interaction domain, i.e., P26 and P27 on the N-terminal side and SU2 on the C-terminal side, interfered with HSPG binding in a dose-dependent manner (Fig. 4). HSPG binding was blocked by treatment with peptide SU2 corresponding to the C-terminal side of TCA 34TF10 V3 but not with P28 corresponding to a similar region of FS PPR V3 (Table 1). SU2 is three amino acids (QRN) longer on the N-terminal end than P28. However, this three-amino-acid region, present in the context of 9 other peptides corresponding to the V3 tip region (Table 1), had no significant effect on HSPG binding. The data suggested that inhibition was mainly caused by the variant amino acid residues located at positions 407 and 409, which is also consistent with previous studies on CrFK tropism determinants (35, 49, 53, 57). P26 and P27 from the N-terminal side of V3 were more potent inhibitors than the C-terminal peptide (Table 1 and Fig. 4); P26 inhibited at around 50%, even at 5 μg/ml (Fig. 4). The combination of P26 and SU2 demonstrated an additive inhibition of HSPG binding by either PPRcr SU (Fig. 4A) or 34TF10 SU (Fig. 4B) in a dose-dependent manner. Thus, the findings are consistent with contributions of sequences from both N- and C-terminal sides of V3 for HSPG binding.

V3 peptides block entry of FIV-34TF10 into G355-5 cells. The above assays measured SU binding to HSPG on target cells. In order to equate binding with ability to enter the cells, we employed the same set of V3 peptides to block virus entry *ex vivo* in single-round infections of G355-5 cells by pseudovirons pseudotyped with 34TF10 Env (Fig. 5) or PPRcr Env (data not shown). Both heparin and AMD3100 blocked entry,

TABLE 1. Sequences of V3 peptides and their abilities to interfere with SU-Fc binding to HSPG in G355-5 cells[a]

Peptide[b]	Origin	Sequence	Inhibition	
			PPRcr	34TF10
V3	PPR	CQRTQSQPGTWIRTISSWRQKNRWEWRPDFESEKVKISLQC	++++	++++
P26	PPR	CQRTQSQPGTWIRTISSWRQKN	+++++	+++++
P27	PPR	TWIRTISSWRQKN	+++	++++
N190	PPR	SSWRQKNRWEWRPDF	+	−
N212	34TF10	SSWKQRNRWEWRPDF	+	−
N43	34TF10	SSWKQRNRWEWR	++	++
N158	34TF10	SSWKQRNRWEW	+	−
N44	34TF10	SSWKQRNRW	++	++
N156	34TF10	SWKQRNRWEWR	−	−
N157	34TF10	WKQRNRWEWR	−	−
N45	34TF10	KQRNRWEWRPDF	+	−
N160	34TF10	QRNRWEWRPDF	−	−
N161	34TF10	RNRWEWRPDF	−	−
N46	PPR/34TF10[d]	NRWEWRPDF	−	−
P28	PPR	RWEWRPDFESEKVKISLQC	−	−
SU2	34TF10	QRNRWEWRPDFKSKKVKISLPC	+++[c]	+++[c]

[a] Percent inhibition was calculated as previously described and is expressed as follows: +++++, 85 to 100% inhibition; ++++, 70 to 85%; +++, 50 to 70%; ++, 30 to 50%; +, 15 to 30%; −, 0 to 15%.
[b] All peptides were used at 50-μg/ml final concentrations.
[c] The inhibition ratio would be increased to greater than 85% if a higher concentration of 100 μg/ml was used.
[d] The origin of the peptide whose sequence is the same in PPR and 34TF10 was labeled as PPR/34TF10.

consistent with the involvement of both HSPG and CXCR4 interactions for entry by beta-galactosidase-expressing particles bearing 34TF10 SU. In accordance with the binding data (Table 1), full-length V3 peptide demonstrated greater than 70% inhibition of entry (Fig. 5). Likewise, peptides coinciding with the N-terminal side (P26 and P27) and the tip region (N190, N212, N43, N158, and N44) of V3 all inhibited entry by 50 to 95%. Blocking by tip region peptides has been shown to occur via inhibition of CXCR4 entry receptor interactions (20, 52). Peptide SU2 corresponding to the C-terminal side of 34TF10 V3 also blocked infection but was less efficient than mimics of either the N-terminal side or tip regions of V3 targeting CXCR4 binding, with a 30% inhibition ratio at similar peptide concentrations (Fig. 5). Higher inhibition ratios could be obtained when higher peptide concentrations were employed (data not shown). P28, a peptide corresponding to the C-terminal side of FS PPR V3, inhibited less than 10%. Other peptides corresponding to portions of the tip region that do not include the CXCR4 interaction domain (i.e., N156, 157, N45, N160, N161, and N46) did not significantly block entry.

Fine mapping of the V3 region required for interaction with HSPG. Comparison of the sequences of FS and TCA envelope proteins (Fig. 1), particularly those of FIV-PPR and FIV-PPRcr, revealed discrete differences that are apparently responsible for the distinct binding phenotypes observed between these two isolates. In particular, PPRcr had a specific change of glutamate to lysine at position 407 and 34TF10 contains two variant lysine residues (407 and 409) relative to FIV-PPR, within the V3 loop (Fig. 1). However, PPRcr also had a change of lysine to glutamate at position 412 (Fig. 1), thus maintaining the same net charge on the V3 region. We replaced Lys407 Lys409, Lys410, and Lys412 in 34TF10 SU with glutamic acid, alone and in various combinations, and then tested the resulting mutant virions for ability to enter G355-5 ($HSPG^{High}$ $CD134^{Neg}$ $CXCR4^{Low}$), 3201 ($CXCR4^{High}$ $HSPG^{Neg}$ $CD134^{Neg}$), and 104-C1 ($CD134^{High}$ $HSPG^{Low}$ $CXCR4^{Low}$) cells (Table 2). We focused on the N-terminal side of V3, since peptides corresponding to this region were more potent inhibitors than the C-terminal peptides. In addition, positively charged residues such as Arg379 and Arg389 are highly conserved in over 200 FIV envelope sequences. Entry facilitated by wild-type 34TF10 SU was arbitrarily set at 100%, and the other entry data were normalized to this value. An arbitrary value of 30% or less relative to entry facilitated by 34TF10 Env (bold numbers in Table 2) was set as significant entry reduction. The results, summarized in Table 2, show that Arg379Glu and Arg389Glu lost virtually all capacity for entry and expression of beta-galactosidase on all the tested cell lines (Table 2), indicating that an acidic amino acid residue at either of these two positions will cause the loss of SU interaction with all receptors. Of interest, when these two positions were replaced with hydrophobic, polar uncharged, or basic amino acid residues, all mutant virions retained greater than 40% capacity to enter 3201 or 104-C1 cells and the three mutants at position 389 retained more than 80% of control-level infectivity. However, these same mutant virions lost the ability to infect G355-5 cells. Even if the same type of basic residue was introduced, the entry ability was still less than 30%, suggesting that Arg379 and Arg389 are crucial for HSPG interaction. Thus, it is probable that not only the electrostatic attraction between the basic N-terminal side of V3 and the acidic HSPG ectodomains but also a steric effect or conformation of amino acid residues around the V3 region of SU plays important roles in facilitating HSPG interactions.

In contrast, substitution of positively charged residues on the C-terminal side of V3 yielded more complicated results. For entry into G355-5 cells, the single substitutions of Lys407, Lys409, Lys410, and Lys412 resulted in only modest reductions in infectivity, while double substitutions had greater effects. Thus, it is probable that this cluster of amino acids acts cooperatively to form a single HSPG binding domain. Interestingly, the Lys407Glu mutant maintained wild-type entry levels on

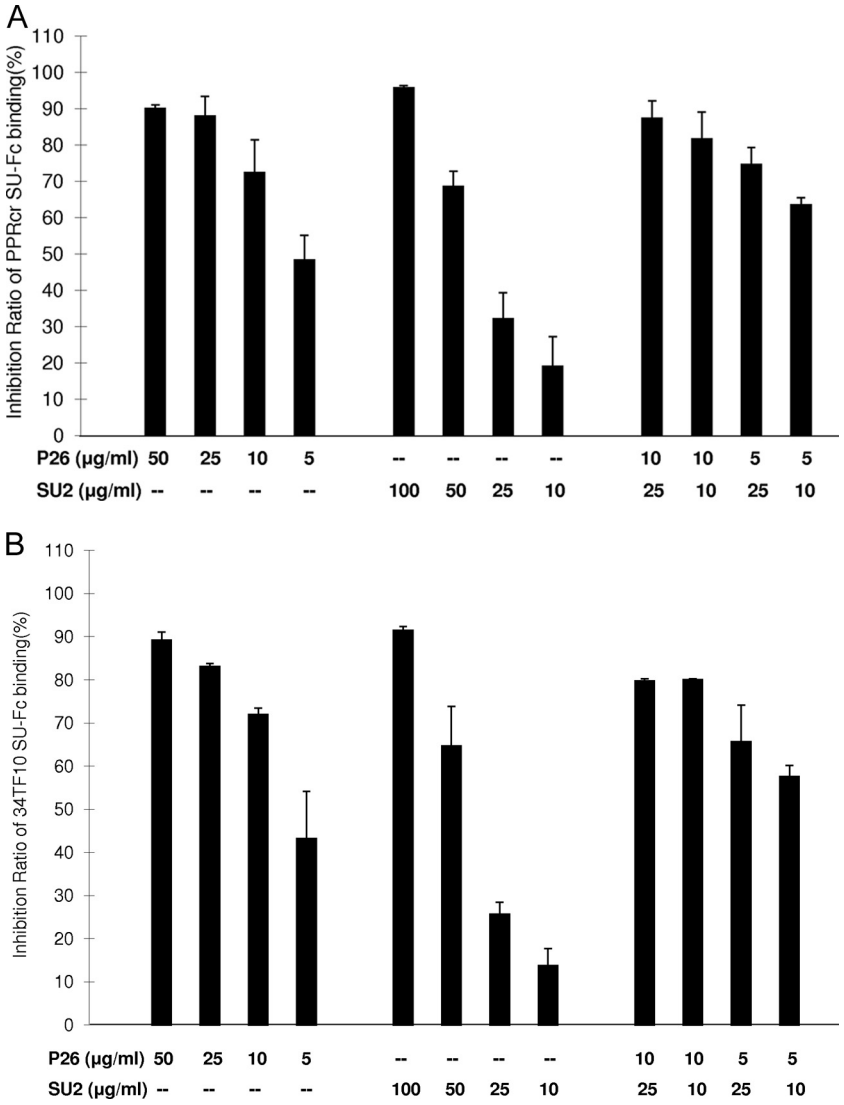

FIG. 4. P26 and SU2 peptides interfere with PPRcr and 34TF10 SU-Fc binding to HSPG in a dose-dependent manner. G355-5 cells were pretreated with P26 or SU2 peptide, alone or in combination, at 4°C for 30 min, and then the cells were spun down to remove the peptides and washed twice. Five hundred nanograms of PPRcr SU-Fc (A) or 34TF10 (B) was added to cells and incubated at 4°C for 45 min. After washing, SU binding was monitored by FACS analysis as described for Fig. 2. When treated separately, P26 was used at 50, 25, 10, and 5 μg/ml as final concentrations and SU2 was used at 100, 50, 25, and 10 μg/ml. When combined, P26 was used at 5 and 10 μg/ml and SU2 was used at 10 and 25 μg/ml. Percent inhibition was calculated as described in Materials and Methods. Results are means ± standard deviations for three independent determinations.

G355-5 cells but was diminished by approximately 80 to 90% for entry into 3201 cells and 104-C1 cells. In contrast, Lys409Glu, Lys410Glu, and Lys412Glu mutants had slightly greater ability to infect 3201 or 104-C1 cells than G355-5 cells (Table 2). The double mutants involving various combinations of the latter three mutations gave mixed results. Some combinations, such as Lys407Glu/Lys409Glu, showed low levels of entry equivalent to values noted with the most damaging mutation on G355-5 or 3201 cells but maintained approximately 50% entry efficiency on 104-C1 cells. On the other hand, the combination Lys407Glu/Lys410Glu retained 50% entry efficiency on G355-5 cells, whereas the entry capacities on 3201 or 104-C1 cells were less than 30% (Table 2). For both Lys409Glu/Lys410Glu and Lys410Glu/Lys412Glu, the entry efficiency on 3201 or 104-C1 cells was much higher than that on G355-5 cells. These results imply that the introduction of double mutations at these positions induces conformational changes in V3 that alter HSPG association. Such interactions would also explain the involvement of distal amino acids from either side of V3 in the HSPG interaction. The entry capacities of Lys407Glu/Lys412Glu and Lys409Glu/Lys412Glu were at similar levels on the three cell lines.

DISCUSSION

HSPGs are a type of glycosaminoglycan (GAG) that participate in many biological processes (12, 29, 31, 38, 44) through their ability to bind a wide range of proteins. For most viruses

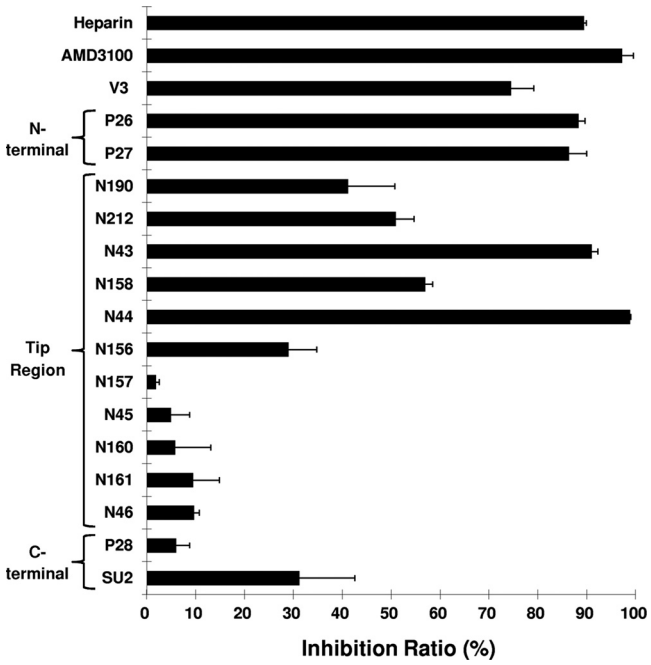

FIG. 5. Neutralization effects of V3 peptides on 34TF10 entry into G355-5 cells. β-Gal-expressing pseudovirions with 34TF10 envelope were produced as described in Materials and Methods. All peptides were preincubated with G355-5 cells at 37°C for 60 min at a final concentration of 25 μg/ml and then cotreated with 34TF10 pseudovirions to perform a single-round infection in G355-5 cells. AMD3100 (1 μg/ml) and heparin (10 μg/ml) were used as positive controls for inhibition of entry. β-Gal assays were performed 48 h after infections. Values for inhibition by peptides, AMD3100, or heparin are percentages of the mean relative luminescence units of 34TF10 entry without any treatment, which is regarded as 100%. Results are means and standard deviations for three independent determinations.

(50), including herpesvirus (1), flavivirus (19), adenovirus (54), papillomavirus (45), and retrovirus family members such as HIV and FIV (3, 7, 10, 43), HSPG can function as a binding receptor or auxiliary attachment factor for initial virus-cell interactions on certain cell types. Some strains of HIV-1 (15, 18, 36, 42, 43, 55) and FIV (9, 41, 59, 61), in particular strains adapted for productive growth in tissue culture (TCA), may employ HSPG as a primary binding receptor in the absence of the primary binding receptor used by field strains (FS), i.e., CD4 for HIV-1 and CD134 for FIV. We surmise that binding through HSPG increases the effective concentration of virus and thus increases the likelihood of binding to low-abundance entry receptors on cell types such as endothelial and epithelial cells that are rich in HSPG expression but have low levels of CXCR4 and lack the normal virus binding receptor (7, 10).

The extent to which HSPG interactions contribute to infection and spread *in vivo* is unknown but could potentially have important consequences for infectivity, spread, and sequestration of virus in cell compartments other than lymphoid cells. Clearly, the *in vivo* distribution of overt viremia by either FIV or HIV is inconsistent with utilization of HSPG for infection, although the extent to which expression below normal detection levels occurs may be underappreciated. Given the high mutation rate and the observations with TCA isolates *ex vivo*, it is equally clear that either virus could quickly mutate to bind HSPG under the right pressures. These observations imply that there must be substantial *in vivo* selection pressures against HSPG binding isolates; enhanced sensitivity to the host immune surveillance network and a propensity for nonproductive binding to polyanionic components of blood or other tissues are two possibilities. However, there is an apparent penalty in adapting for HSPG binding in that the ability to bind to the normal primary binding receptor, CD134, is markedly reduced (Fig. 5). This may act to limit spread of HSPG binding virus, thus reducing the targeting of T cells. Regardless, given that immunological and/or drug treatment modalities may alter the balance of *in vivo* selective pressures, it is reasonable to propose that such isolates might play a significant role *in vivo* under the proper circumstances.

Understanding the functional role of HSPG-envelope interaction requires the identification of the structural determinants involved in the interaction, on both HSPG and the viral envelope protein. In this report, we characterized HSPG binding motifs on FIV SU and further defined the key amino acid residues required for FIV SU-HSPG interactions.

Two invariant arginine residues, Arg379 and Arg389, on the N-terminal side of V3 are critical for changing binding phenotype, implying discontiguous interactions within the three-dimensional structure around V3 (Fig. 6). The findings are consistent with the report that a highly conserved arginine at position 298 on the N-terminal side of the V3 loop of HIV-1 is critical for binding to HSPG and CCR5 in the HIV studies (5). This observation underscores the close parallels in the envelope structural motifs and probable overall envelope protein structure of these two viruses, in spite of their diverse primary sequences.

Our studies show that TCA FIVs adapted to propagate in

TABLE 2. Entry efficiency of 34TF10 mutants compared with wild type in cells[a]

Strain	Entry ratio (%) for cell line:		
	G355-5	3201	104-C1
Wild type	100.0 ± 0.0	100.0 ± 0.0	100.0 ± 0.0
Mutants			
R379E	**2.1 ± 0.8**	**2.2 ± 0.9**	**4.1 ± 0.7**
R379A	**5.6 ± 0.9**	57.5 ± 9.6	41.6 ± 6.7
R379Q	**1.6 ± 0.5**	84.2 ± 4.7	76.6 ± 0.3
R379K	**6.8 ± 0.5**	55.4 ± 0.2	55.1 ± 16.8
R389E	**1.5 ± 0.9**	**2.4 ± 1.1**	**2.7 ± 0.3**
R389A	**3.5 ± 0.3**	81.7 ± 10.3	98.7 ± 9.8
R389Q	**28.2 ± 1.2**	103.8 ± 3.9	104.5 ± 4.3
R389K	**22.3 ± 3.1**	104.6 ± 6.6	100.3 ± 7.9
K407E	90.3 ± 10.0	**10.3 ± 4.6**	**26.4 ± 6.8**
K409E	89.8 ± 1.8	94.8 ± 3.8	94.7 ± 6.4
K410E	39.7 ± 4.7	71.3 ± 9.8	76.3 ± 2.9
K412E	86.5 ± 5.9	113.6 ± 9.2	111.4 ± 3.8
K407E/K409E	**13.6 ± 0.5**	**5.2 ± 1.0**	55.1 ± 5.1
K407E/K410E	53.0 ± 2.0	**13.6 ± 6.0**	**29.9 ± 8.7**
K407E/K412E	**22.4 ± 6.7**	**7.9 ± 5.3**	**14.3 ± 1.7**
K409E/K410E	47.2 ± 2.5	90.0 ± 1.6	95.9 ± 4.8
K409E/K412E	**29.4 ± 0.4**	**16.4 ± 0.2**	**16.7 ± 1.0**
K410E/K412E	**3.4 ± 2.0**	57.3 ± 1.5	41.3 ± 5.7

[a] Entry facilitated by wild-type 34TF10 SU was arbitrarily set at 100%, and the other entry data were normalized to this value. An arbitrary value of 30% or less relative to entry facilitated by 34TF10 Env (boldface) was set as significant entry reduction.

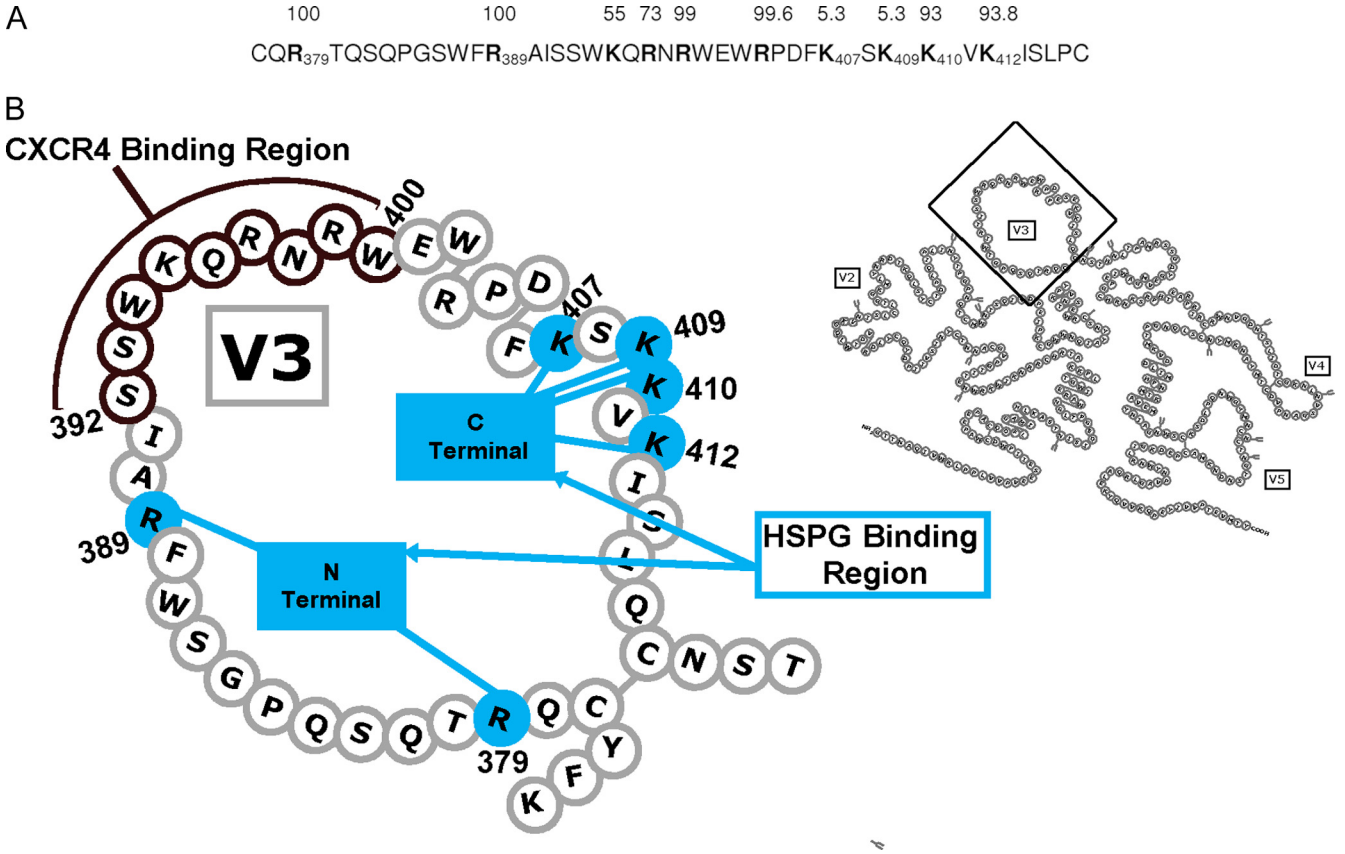

FIG. 6. Schematic representation of V3 in the context of SU. (A) Sequence of the V3 region, with residues relevant to HSPG binding shown in bold. Numbers above the line represent percent conservation in comparing approximately 200 V3 sequences from known FIV isolates. (B) Cartoon showing the CXCR4 and HSPG binding regions defined on FIV V3.

CrFK cells have acquired a set of important mutations within the V3 loop (Fig. 1). Interestingly, we found that a Lys407Glu back mutation in the context of TCA isolate 34TF10 retained the ability to enter G355-5 cells but showed marked reduction in entry to 3201 cells. This implies that over time, TCA-specific mutations that act to not only allow HSPG binding but also optimize binding to CXCR4 occur. Thus, results of changing any one of these mutations can be difficult to predict since the basic amino acid residues on the C-terminal side of V3 work in concert to yield the observed binding phenotype. Overall, the findings suggest a structural interplay between the two sides of the V3 stem that somehow facilitates HSPG interaction (Fig. 6). The sites for HSPG binding comprising distal amino acids are presumably organized in a precise spatial orientation, perhaps similar to the heparin binding domain for human hepatic lipase (63). Hepatic lipase contains two putative heparin binding regions: one consists of residues R310, K312, K314, and R315 at a distal region of the N-terminal domain and the other region is made up of R473, K474, and R476 at the C-terminal end of the molecule (63).

Some previous reports (7, 14, 32, 42) have suggested that the overall positive charge may also influence HSPG binding. However, the study here suggests that the overall electrostatic potential of the V3 loop is not the primary determinant. In addition, it was observed that there is no obvious correlation between the number of basic residues within V3 and the capacity of HIV-1 to bind HSPG (5).

It is important to point out that what we are studying is the acquisition of the ability to productively infect adherent tissue culture cells. In the present study, FS FIV must be able to get into these cells and undergo low-level replication (via CXCR4 alone) in order to adapt and take on the high-titer, rapid growth characteristics of TCA strains. Whether the acquisition of HSPG binding totally supplants the requirement for CD134 (CD4 for HIV) interaction is unclear. Both CrFK and G355-5 express the entry receptor, CXCR4, but lack expression of CD134, so productive infection of these cells requires HSPG interaction. TCA PPRcr SU still binds CD134 on 104-C1 T cells (Fig. 3), but with much less alacrity than does wild-type PPR SU. Both CD134 and HSPG appear to recognize SU tertiary conformation, as evidenced by the discontiguous nature of HSPG binding emphasized above and by similar discontiguous association between SU and CD134 (20, 52). This is in contrast to the contiguous region that binds the entry receptor, CXCR4, which resides at the tip of the V3 loop on both FS and TCA FIV envelope proteins. Both strains are dependent on CXCR4 for cell entry (inhibited by AMD3100), and peptides that block CXCR4 binding at the V3 tip do not block either HSPG (Table 1) or CD134 (20) binding. However, all of

these interactions occur on and around the V3 loop, underscoring the central role of this putative structure in infection.

Our study discloses the characteristics of the HSPG binding motifs of SU and the critical residues responsible for SU-HSPG interaction in the V3 loop of FIV. Furthermore, the discrimination of structural determinants important for HSPG and CXCR4 interaction of FIV SU should aid in understanding FIV Env structure and help define the targets for blocking virus entry and infection.

ACKNOWLEDGMENTS

We thank Ying-Chuan Lin and Yang Hong for valuable comments and Gale Sessions for manuscript preparation.

The project was supported by grant R01 AI25825 from the National Institute of Allergy and Infectious Diseases of the National Institutes of Health. The peptide facility at the M. D. Anderson Cancer Center was supported with funds from NIH grant CA 16672.

REFERENCES

1. **Akhtar, J., and D. Shukla.** 2009. Viral entry mechanisms: cellular and viral mediators of herpes simplex virus entry. FEBS J. **276:**7228–7236.
2. **Andrianov, A. M., and V. G. Veresov.** 2007. Structural analysis of the HIV-1 gp120 V3 loop: application to the HIV-Haiti isolates. J. Biomol. Struct. Dyn. **24:**597–608.
3. **Bobardt, M. D., et al.** 2003. Syndecan captures, protects, and transmits HIV to T lymphocytes. Immunity **18:**27–39.
4. **Cardin, A. D., and H. J. Weintraub.** 1989. Molecular modeling of protein-glycosaminoglycan interactions. Arteriosclerosis **9:**21–32.
5. **de Parseval, A., et al.** 2005. A highly conserved arginine in gp120 governs HIV-1 binding to both syndecans and CCR5 via sulfated motifs. J. Biol. Chem. **280:**39493–39504.
6. **de Parseval, A., U. Chatterji, P. Sun, and J. H. Elder.** 2004. Feline immunodeficiency virus targets activated CD4+ T cells by using CD134 as a binding receptor. Proc. Natl. Acad. Sci. U. S. A. **101:**13044–13049.
7. **de Parseval, A., and J. H. Elder.** 2001. Binding of recombinant feline immunodeficiency virus surface glycoprotein to feline cells: role of CXCR4, cell-surface heparans, and an unidentified non-CXCR4 receptor. J. Virol. **75:**4528–4539.
8. **de Parseval, A., D. L. Lerner, P. Borrow, B. J. Willett, and J. H. Elder.** 1997. Blocking of feline immunodeficiency virus infection by a monoclonal antibody to CD9 is via inhibition of virus release rather than interference with receptor binding. J. Virol. **71:**5742–5749.
9. **de Parseval, A., S. Ngo, P. Sun, and J. H. Elder.** 2004. Factors that increase the effective concentration of CXCR4 dictate feline immunodeficiency virus tropism and kinetics of replication. J. Virol. **78:**9132–9143.
10. **de Parseval, A., S. V. Su, J. H. Elder, and B. Lee.** 2004. Specific interaction of feline immunodeficiency virus surface glycoprotein with human DC-SIGN. J. Virol. **78:**2597–2600.
11. **Elder, J. H., et al.** 2008. Molecular mechanisms of FIV infection. Vet. Immunol. Immunopathol. **123:**3–13.
12. **Esko, J. D., and S. B. Selleck.** 2002. Order out of chaos: assembly of ligand binding sites in heparan sulfate. Annu. Rev. Biochem. **71:**435–471.
13. **Esko, J. D., T. E. Stewart, and W. H. Taylor.** 1985. Animal cell mutants defective in glycosaminoglycan biosynthesis. Proc. Natl. Acad. Sci. U. S. A. **82:**3197–3201.
14. **Fouchier, R. A., et al.** 1992. Phenotype-associated sequence variation in the third variable domain of the human immunodeficiency virus type 1 gp120 molecule. J. Virol. **66:**3183–3187.
15. **Gallay, P.** 2004. Syndecans and HIV-1 pathogenesis. Microbes Infect. **6:**617–622.
16. **Geijtenbeek, T. B., A. Engering, and Y. Van Kooyk.** 2002. DC-SIGN, a C-type lectin on dendritic cells that unveils many aspects of dendritic cell biology. J. Leukoc. Biol. **71:**921–931.
17. **Gout, E., G. Schoehn, D. Fenel, H. Lortat-Jacob, and P. Fender.** 2010. The adenovirus type 3 dodecahedron's RGD loop comprises an HSPG binding site that influences integrin binding. J. Biomed. Biotechnol. **2010:**541939.
18. **Hamon, M., et al.** 2004. A syndecan-4/CXCR4 complex expressed on human primary lymphocytes and macrophages and HeLa cell line binds the CXC chemokine stromal cell-derived factor-1 (SDF-1). Glycobiology **14:**311–323.
19. **Hilgard, P., and R. Stockert.** 2000. Heparan sulfate proteoglycans initiate dengue virus infection of hepatocytes. Hepatology **32:**1069–1077.
20. **Hu, Q. Y., et al.** 2010. Fine definition of the CXCR4-binding region on the V3 loop of feline immunodeficiency virus surface glycoprotein. PLoS One **5:**e10689.
21. **Johnson, G., C. Swart, and S. W. Moore.** 2008. Interaction of acetylcholinesterase with the G4 domain of the laminin alpha1-chain. Biochem. J. **411:**507–514.
22. **Johnston, J. C., et al.** 1999. Minimum requirements for efficient transduction of dividing and nondividing cells by feline immunodeficiency virus vectors. J. Virol. **73:**4991–5000.
23. **Jones, K. S., C. Petrow-Sadowski, D. C. Bertolette, Y. Huang, and F. W. Ruscetti.** 2005. Heparan sulfate proteoglycans mediate attachment and entry of human T-cell leukemia virus type 1 virions into CD4+ T cells. J. Virol. **79:**12692–12702.
24. **Kang, B. S., et al.** 2003. PDZ tandem of human syntenin: crystal structure and functional properties. Structure **11:**459–468.
25. **Kuschert, G. S., et al.** 1998. Identification of a glycosaminoglycan binding surface on human interleukin-8. Biochemistry (Mosc.) **37:**11193–11201.
26. **Lerner, D. L., and J. H. Elder.** 2000. Expanded host cell tropism and cytopathic properties of feline immunodeficiency virus strain PPR subsequent to passage through interleukin-2-independent T cells. J. Virol. **74:**1854–1863.
27. **Lerner, D. L., C. K. Grant, A. de Parseval, and J. H. Elder.** 1998. FIV infection of IL-2-dependent and -independent feline lymphocyte lines: host cells range distinctions and specific cytokine upregulation. Vet. Immunol. Immunopathol. **65:**277–297.
28. **Levy, P., et al.** 1990. Altered expression of proteoglycans in E1A-immortalized rat fetal intestinal epithelial cells in culture. Cancer Res. **50:**6716–6722.
29. **Liu, J., and S. C. Thorp.** 2002. Cell surface heparan sulfate and its roles in assisting viral infections. Med. Res. Rev. **22:**1–25.
30. **Lortat-Jacob, H., A. Grosdidier, and A. Imberty.** 2002. Structural diversity of heparan sulfate binding domains in chemokines. Proc. Natl. Acad. Sci. U. S. A. **99:**1229–1234.
31. **Lyon, M., and J. T. Gallagher.** 1998. Bio-specific sequences and domains in heparan sulphate and the regulation of cell growth and adhesion. Matrix Biol. **17:**485–493.
32. **Moulard, M., et al.** 2000. Selective interactions of polyanions with basic surfaces on human immunodeficiency virus type 1 gp120. J. Virol. **74:**1948–1960.
33. **Mulloy, B., and R. J. Linhardt.** 2001. Order out of complexity—protein structures that interact with heparin. Curr. Opin. Struct. Biol. **11:**623–628.
34. **Oh, E. S., J. R. Couchman, and A. Woods.** 1997. Serine phosphorylation of syndecan-2 proteoglycan cytoplasmic domain. Arch. Biochem. Biophys. **344:**67–74.
35. **Olmsted, R. A., V. M. Hirsch, R. H. Purcell, and P. R. Johnson.** 1989. Nucleotide sequence analysis of feline immunodeficiency virus: genome organization and relationship to other lentiviruses. Proc. Natl. Acad. Sci. U. S. A. **86:**8088–8092.
36. **Patel, M., et al.** 1993. Cell-surface heparan sulfate proteoglycan mediates HIV-1 infection of T-cell lines. AIDS Res. Hum. Retroviruses **9:**167–174.
37. **Pedersen, N. C., E. W. Ho, M. L. Brown, and J. K. Yamamoto.** 1987. Isolation of a T-lymphotropic virus from domestic cats with an immunodeficiency-like syndrome. Science **235:**790–793.
38. **Perrimon, N., and M. Bernfield.** 2000. Specificities of heparan sulphate proteoglycans in developmental processes. Nature **404:**725–728.
39. **Phillips, T. R., et al.** 1990. Comparison of two host cell range variants of feline immunodeficiency virus. J. Virol. **64:**4605–4613.
40. **Podell, M., W. R. Buck, K. A. Hayes, M. A. Gavrilin, and L. E. Mathes.** 2002. Animal models of retroviral encephalopathies: feline model. Curr. Protoc. Neurosci. **9:**9.9.1–9.9.30.
41. **Richardson, J., et al.** 1999. Shared usage of the chemokine receptor CXCR4 by primary and laboratory-adapted strains of feline immunodeficiency virus. J. Virol. **73:**3661–3671.
42. **Roderiquez, G., et al.** 1995. Mediation of human immunodeficiency virus type 1 binding by interaction of cell surface heparan sulfate proteoglycans with the V3 region of envelope gp120-gp41. J. Virol. **69:**2233–2239.
43. **Saphire, A. C., M. D. Bobardt, Z. Zhang, G. David, and P. A. Gallay.** 2001. Syndecans serve as attachment receptors for human immunodeficiency virus type 1 on macrophages. J. Virol. **75:**9187–9200.
44. **Sasisekharan, R., Z. Shriver, G. Venkataraman, and U. Narayanasami.** 2002. Roles of heparan-sulphate glycosaminoglycans in cancer. Nat. Rev. Cancer. **2:**521–528.
45. **Shafti-Keramat, S., et al.** 2003. Different heparan sulfate proteoglycans serve as cellular receptors for human papillomaviruses. J. Virol. **77:**13125–13135.
46. **Shepherd, T. R., et al.** 2010. The Tiam1 PDZ domain couples to Syndecan1 and promotes cell-matrix adhesion. J. Mol. Biol. **398:**730–746.
47. **Shih, P. C., et al.** 2009. A turn-like structure "KKPE" segment mediates the specific binding of viral protein A27 to heparin and heparan sulfate on cell surfaces. J. Biol. Chem. **284:**36535–36546.
48. **Shimojima, M., et al.** 2004. Use of CD134 as a primary receptor by the feline immunodeficiency virus. Science **303:**1192–1195.
49. **Siebelink, K. H., J. A. Karlas, G. F. Rimmelzwaan, A. D. Osterhaus, and M. L. Bosch.** 1995. A determinant of feline immunodeficiency virus involved in Crandell feline kidney cell tropism. Vet. Immunol. Immunopathol. **46:**61–69.
50. **Spillmann, D.** 2001. Heparan sulfate: anchor for viral intruders? Biochimie **83:**811–817.
51. **Stringer, S. E., et al.** 2002. Characterization of the binding site on heparan sulfate for macrophage inflammatory protein 1alpha. Blood **100:**1543–1550.
52. **Sundstrom, M., et al.** 2008. Mapping of the CXCR4 binding site within

variable region 3 of the feline immunodeficiency virus surface glycoprotein. J. Virol. **82:**9134–9142.
53. **Talbott, R. L., et al.** 1989. Nucleotide sequence and genomic organization of feline immunodeficiency virus. Proc. Natl. Acad. Sci. U. S. A. **86:**5743–5747.
54. **Tuve, S., et al.** 2008. Role of cellular heparan sulfate proteoglycans in infection of human adenovirus serotype 3 and 35. PLoS Pathog. **4:**e1000189.
55. **Ugolini, S., I. Mondor, and Q. J. Sattentau.** 1999. HIV-1 attachment: another look. Trends Microbiol. **7:**144–149.
56. **Uhl, E. W., M. Martin, J. K. Coleman, and J. K. Yamamoto.** 2008. Advances in FIV vaccine technology. Vet. Immunol. Immunopathol. **123:**65–80.
57. **Verschoor, E. J., et al.** 1995. A single mutation within the V3 envelope neutralization domain of feline immunodeficiency virus determines its tropism for CRFK cells. J. Virol. **69:**4752–4757.
58. **Vives, R. R., et al.** 2004. A novel strategy for defining critical amino acid residues involved in protein/glycosaminoglycan interactions. J. Biol. Chem. **279:**54327–54333.
59. **Willett, B. J., et al.** 1998. The second extracellular loop of CXCR4 determines its function as a receptor for feline immunodeficiency virus. J. Virol. **72:**6475–6481.
60. **Willett, B. J., and M. J. Hosie.** 2008. Chemokine receptors and costimulatory molecules: unravelling feline immunodeficiency virus infection. Vet. Immunol. Immunopathol. **123:**56–64.
61. **Willett, B. J., et al.** 1997. Shared usage of the chemokine receptor CXCR4 by the feline and human immunodeficiency viruses. J. Virol. **71:**6407–6415.
62. **Yamashita, H., K. Beck, and Y. Kitagawa.** 2004. Heparin binds to the laminin alpha4 chain LG4 domain at a site different from that found for other laminins. J. Mol. Biol. **335:**1145–1149.
63. **Yu, W., and J. S. Hill.** 2006. Mapping the heparin-binding domain of human hepatic lipase. Biochem. Biophys. Res. Commun. **343:**659–665.